Preventing diet-induced obesity in mice by adipose tissue transformation and angiogenesis using targeted nanoparticles

Yuan Xue[a,1], Xiaoyang Xu[a,b,c,1], Xue-Qing Zhang[b], Omid C. Farokhzad[b,d,2], and Robert Langer[a,2]

[a]The David H. Koch Institute for Integrative Cancer Research, Massachusetts Institute of Technology, Cambridge, MA 02139; [b]Laboratory of Nanomedicine and Biomaterials, Department of Anesthesiology, Brigham and Women's Hospital, Harvard Medical School, Boston, MA 02115; [c]Department of Chemical, Biological, and Pharmaceutical Engineering, New Jersey Institute of Technology, Newark, NJ 07102; and [d]King Abdulaziz University, Jeddah 21589, Saudi Arabia

Contributed by Robert Langer, March 28, 2016 (sent for review January 12, 2016; reviewed by and Sangyong Jon and Liangfang Zhang)

The incidence of obesity, which is recognized by the American Medical Association as a disease, has nearly doubled since 1980, and obesity-related comorbidities have become a major threat to human health. Given that adipose tissue expansion and transformation require active growth of new blood vasculature, angiogenesis offers a potential target for the treatment of obesity-associated disorders. Here we construct two peptide-functionalized nanoparticle (NP) platforms to deliver either Peroxisome Proliferator-Activated Receptor gamma (PPARgamma) activator rosiglitazone (Rosi) or prostaglandin E2 analog (16,16-dimethyl PGE2) to adipose tissue vasculature. These NPs were engineered through self-assembly of a biodegradable triblock polymer composed of end-to-end linkages between poly(lactic-coglycolic acid)-*b*-poly(ethylene glycol) (PLGA-*b*-PEG) and an endothelial-targeted peptide. In this system, released Rosi promotes both transformation of white adipose tissue (WAT) into brown-like adipose tissue and angiogenesis, which facilitates the homing of targeted NPs to adipose angiogenic vessels, thereby amplifying their delivery. We show that i.v. administration of these NPs can target WAT vasculature, stimulate the angiogenesis that is required for the transformation of adipose tissue, and transform WAT into brown-like adipose tissue, by the up-regulation of angiogenesis and brown adipose tissue markers. In a diet-induced obese mouse model, these angiogenesis-targeted NPs have inhibited body weight gain and modulated several serological markers including cholesterol, triglyceride, and insulin, compared with the control group. These findings suggest that angiogenesis-targeting moieties with angiogenic stimulator-loaded NPs could be incorporated into effective therapeutic regimens for clinical treatment of obesity and other metabolic diseases.

nanoparticle | targeting | angiogenesis | adipose tissue | transformation

Human adipose tissues undergo constant expansion and regression, which are both dependent on angiogenesis (1–3). Recent evidence reveals that adipose tissue development is associated with microvessel growth and requires vascular remodeling (4). In addition, the modulation of blood vasculature can directly affect adipose tissue metabolism (3, 5, 6). The crosstalk among many types of cells including adipocytes, endothelial cells (ECs), and stromal cells is mediated by multiple angiogenic factors that play pivotal roles in cooperatively modulating adipogenesis (2). Adipogenesis and angiogenesis are temporally and spatially coupled processes whose concomitance indicates that targeting the adipose tissue vasculature may constitute a viable therapeutic intervention for obesity.

Massive expansion of adipose tissues such as white adipose tissue (WAT) leads to obesity, which has become a major threat to human health throughout the world (7). Current therapeutic approaches to obesity include restriction of calorie intake through various diet regimens; increased caloric expenditure through physical activity and exercise; pharmacologic options such as Orlistat, Lorcaserin, and Phentermine-topiramate; and surgical interventions including gastric bypass procedures (8). Few therapeutic agents are available for treating obesity in the clinic due to the complex interplay of genetic, environmental, and cultural factors (9). Previous studies have shown that modulations against vascular development in adipose tissues could alter tissue metabolism and inhibit the development of obesity in mice as well as monkeys (3, 5, 10). However, treating obesity with antiangiogenesis therapy has been hindered by the fact that energy expenditure in certain types of adipose tissue is critically dependent on angiogenesis (6), and an approach to differentially deliver an antiangiogenic agent to the adipose tissue has remained largely elusive. WAT stores energy in the form of fatty acids, whereas brown adipose tissue (BAT) generates heat through nonshivering thermogenesis. Upon the discovery of human BAT, the transformation of WAT into BAT as well as activation of BAT energy expenditure capacity has become an alternative strategy for obesity treatment (4, 11, 12). Here we hypothesize that adipose tissue transformation from energy storage status (WAT) into energy expenditure status (BAT), coupled with stimulation of angiogenesis, is an effective approach for obesity treatment.

Significance

Obesity has been recognized by the American Medical Association to be a disease affecting significant portions of the population and is related to an expansion and proliferation of white adipose tissue (WAT) in the body. The primary function of WAT is to store energy, whereas brown adipose tissue (BAT) generates heat through energy expenditure. Transforming WAT into BAT is of tremendous interest for obesity treatment. Herein, we describe a targeted nanoparticle approach encapsulating either a PPARgamma activator or a prostaglandin E2 analog, each of which induces adipose tissue transformation and angiogenesis, facilitating the transformation of WAT into BAT. Targeted nanoparticles show antiobesity effects compared with free drug and the nontargeted nanoparticle controls in a mouse model.

Author contributions: Y.X., X.X., X.-Q.Z., O.C.F., and R.L. designed research; Y.X., X.X., and X.-Q.Z. performed research; Y.X., X.X., X.-Q.Z., O.C.F., and R.L. analyzed data; and Y.X., X.X., X.-Q.Z., O.C.F., and R.L. wrote the paper.

Reviewers: S.J., Korea Advanced Institute of Science and Technology; and L.Z., University of California, San Diego.

Conflict of interest statement: O.C.F. and R.L. disclose their financial interest in BIND Therapeutics, Selecta Biosciences, and Tarveda Therapeutics, three biotechnology companies developing nanoparticle technologies for medical applications. BIND, Selecta, and Tarveda did not support the aforementioned research, and currently, these companies have no rights to any technology or intellectual property developed as part of this research. The rest of the authors declare no conflict of interest.

[1]Y.X. and X.X. contributed equally to this work.

[2]To whom correspondence may be addressed. Email: ofarokhzad@zeus.bwh.harvard.edu or rlanger@mit.edu.

This article contains supporting information online at www.pnas.org/lookup/suppl/doi:10.1073/pnas.1603840113/-/DCSupplemental.

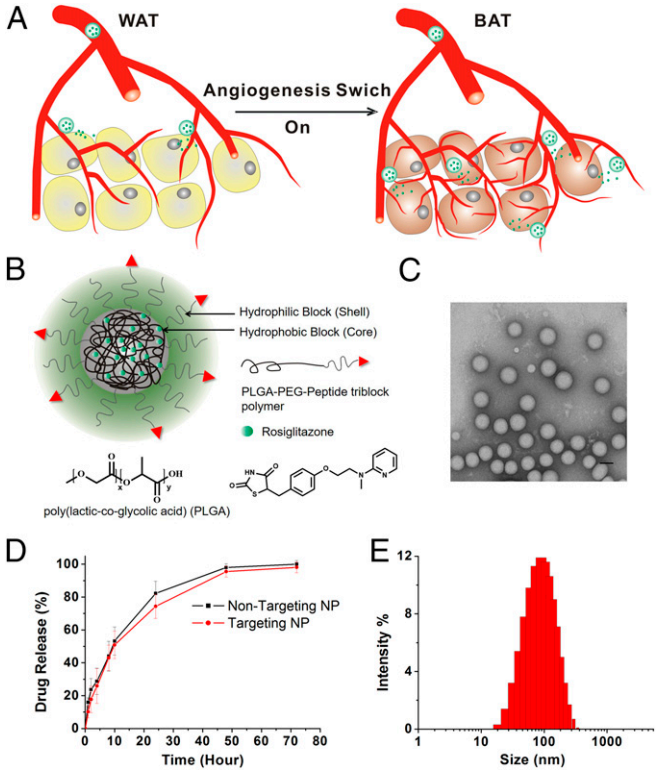

Fig. 1. NP design and characterization. (*A*) A schematic representation of the WAT browning process through a positive feedback drug delivery system. Released Rosi and PGE2 promote transformation of WAT into brown-like adipose tissue and stimulate angiogenesis. This facilitates the homing of targeted NPs to adipose angiogenic vessels, thereby amplifying their delivery and hence expediting the WAT browning process. (*B*) Chemical structure of PLGA-b-PEG-Peptide/Rosiglitazone NPs (NPs). The particle consists of two components: (*i*) an outer PEG surface with a targeting peptide iRGD or P3, which can bind to angiogenic vessels through Integrinavb3/b5 receptors and WAT vasculature through the membrane protein prohibitin, respectively, and (*ii*) a PLGA hydrophobic core that serves two functions: first, acting as a polymer matrix loaded with Rosiglitazone, and second, promoting Rosiglitazone molecule retention inside the NP core and controlling drug release. Nontargeted and targeted NPs encapsulating Rosiglitazone were formulated via a single-step emulsion method. (*C*) Representative TEM image of the iRGD-NP-Rosi. (*D*) In vitro release profile of Rosiglitazone from NP-Rosi and iRGD-NP-Rosi. (*E*) Size distribution of the iRGD-NP-Rosi measured by dynamic light scattering.

Numerous weight loss drugs have been abandoned because of undesired side effects (9) resulting from broad targeting spectrums that affect multiple organs and tissues. One advantage of nanoparticle technologies in the treatment of various diseases stems from their ability to passively or actively target the organs or tissues of interest. In addition, targeted nanoparticles have shown promising clinical benefits in cancer therapy (13). Herein we describe polymeric nanoparticles using a poly(lactide-coglycolide)-*b*-poly(ethylene glycol) (PLGA-*b*-PEG) copolymer, which consists of a hydrophobic core loaded with therapeutic compounds, a hydrophilic PEG corona, and a targeting peptide that binds to antigens preferentially expressed on the endothelium of angiogenic vasculature (Fig. 1*A*). To examine the concept, we encapsulate within the NP rosiglitazone (Rosi), a PPARgamma activator, and prostaglandin E2 analog (16,16-dimethyl PGE2, PGE2), either of which could induce adipose tissue transformation and angiogenesis. Rosi has been reported to stimulate PPAR activity, which leads not only to adipose tissue transformation by increasing the expression levels of uncoupling proteins but also activates angiogenesis in adipose tissue by elevating expression levels of VEGF and angiopoietin-like 4 (14–16). PGE2 has been shown to activate the prostaglandin receptor, which promotes adipose tissue transformation by increasing the expression of Uncoupling protein 1 (UCP1) (17). We show that peptide-conjugated NPs effectively deliver Rosi and PGE2 into adipose tissues while minimizing adverse effects on other tissues. We confirm that drug-loaded targeted NPs up-regulate angiogenic and BAT markers, activate angiogenesis (as represented by intensified vascularization), and facilitate the transformation of WAT into BAT. Furthermore, using a diet-induced obesity (DIO) mouse model, we demonstrate that Rosi-loaded and peptide-functionalized NPs (peptide-NP-Rosi) inhibit weight gain as well as down-regulate several serological markers such as cholesterol, triglycerides, and insulin. These results support our hypothesis that coupling adipose tissue transformation with stimulation of angiogenesis is a potentially effective approach for obesity treatment. The vasculature-targeting approach greatly accelerates adipose tissue transformation through stimulation of angiogenesis, which has not been observed previously using free drug or untargeted NPs. This design rationale has produced promising results in reducing obesity by taking advantage of vasculature-targeted nanomedicine coupled with angiogenesis stimulation, opening potential new avenues in developing therapeutic regimens for obesity treatment.

Results

Synthesis of Peptide-Conjugated NPs. Two adipose vasculature-targeted peptides, iRGD and P3, were covalently conjugated to PLGA-PEG-MAL via the free thiols of the peptides' C-terminal using maleimide chemistry. The iRGD (CRGDK/RGPD/EC)

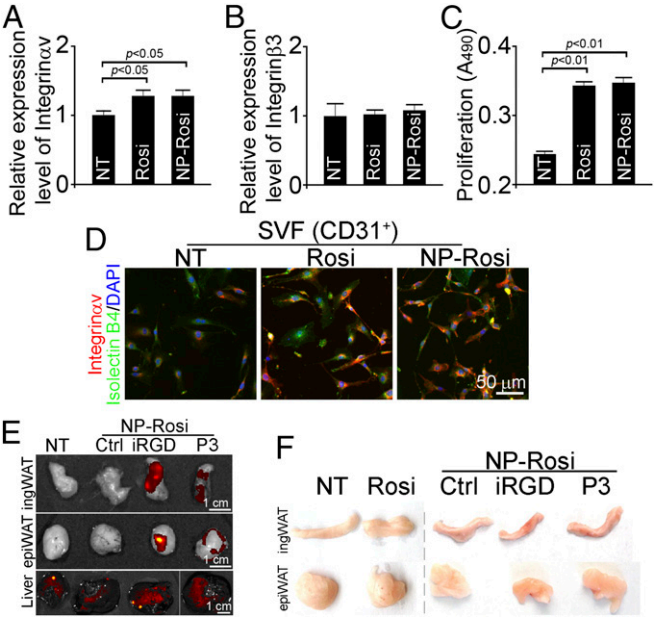

Fig. 2. NPs stimulate angiogenesis in vitro and target to adipose tissue in vivo. Stromal vascular fragments (SVF) were isolated from inguinal WAT and were treated with free Rosi and NP-encapsulated Rosi (NP-Rosi). (*A*) Relative expression levels of Integrinαv in SVF from inguinal WAT (ingWAT) were measured by qRT-PCR ($n = 3$ per group). (*B*) Relative expression levels of Integrinβ3 in SVF from ingWAT were measured by qRT-PCR PCR ($n = 3$ per group). (*C*) Proliferation of SVF from ingWAT induced by Rosi and NP-Rosi treatments PCR ($n = 6$ per group). (*D*) $CD31^+$ SVF was sorted and stained with Integrinαv antibody (red), Isolectin B4 (green), and DAPI (blue). C57BL/6 mice were treated with Rosi, NP-Rosi, iRGD-NP-Rosi, or P3-NP-Rosi for 2 wk ($n = 3$). (Scale bar, 50 μm.) (*E*) IngWAT, epiWAT, and livers were dissected, and representative samples were imaged under the IVIS imaging system. (Scale bars, 1 cm.) (*F*) Inguinal WAT and epididymal WAT were dissected, and representative samples were photographed.

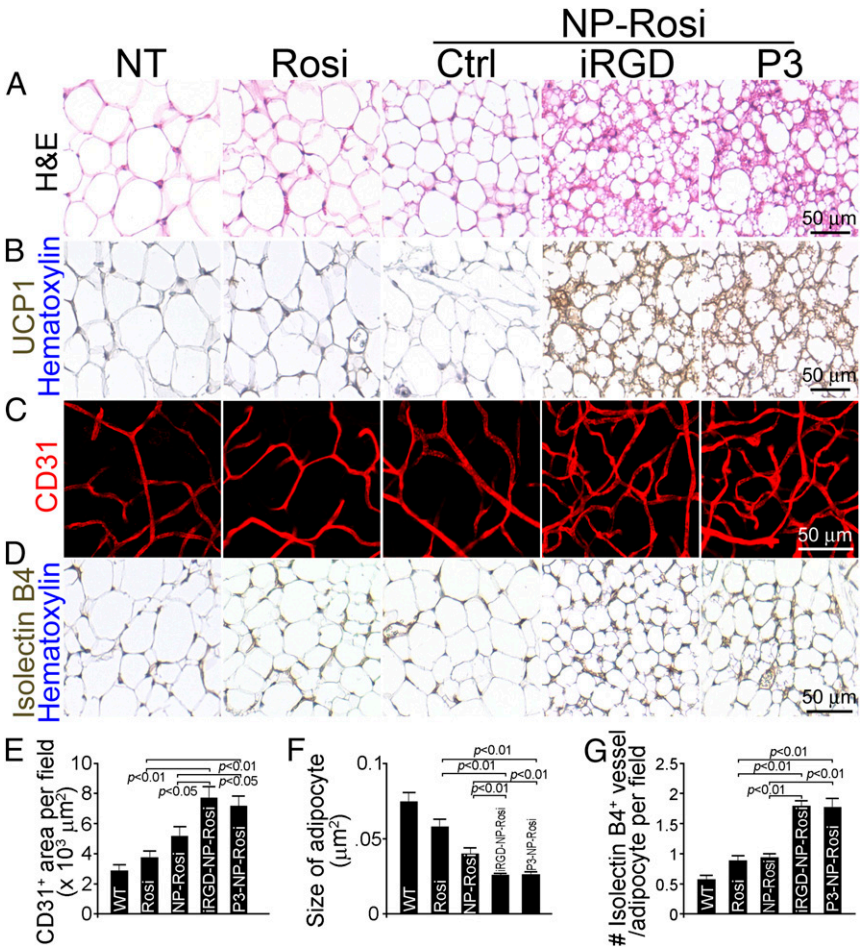

Fig. 3. IRGD- and P3-NP-Rosi induced adipose tissue transformation and angiogenesis in vivo. C57BL/6 mice received treatments with Rosi, NP-Rosi, iRGD-NP-Rosi, or P3-NP-Rosi for 15 d. (*A*) Sections of ingWAT were stained with hematoxylin and eosin to demonstrate the general histology of adipose tissues. (Scale bar, 50 μm.) (*C*) Portions of ingWAT were immune-stained with anti-CD31 antibody (red), and 3D images were captured under a confocal microscope. (Scale bar, 50 μm.) (*D*) Sections of ingWAT were stained with Isolectin B4 (brown) and hematoxylin (blue). (Scale bar, 50 μm.) (*B*) Sections of ingWAT were stained with anti-UCP1 antibody (brown) and hematoxylin (blue). (Scale bar, 50 μm.) (*E*) Density of $CD31^+$ blood vessel area per optical field was quantified from confocal images. Data represent means ± SEM from nine samples from four mice in each group. (*F*) Quantification of average size of adipocytes from different treatment groups. Data represent means ± SEM from nine samples from four mice in each group. (*G*) Quantification of numbers of isolectin-positive vessels per adipocyte of ingWAT. Data represent means ± SEM from nine samples from four mice in each group.

peptide has been reported to bind to angiogenic vessels through Integrinαvβ3/β5 receptors and to home the drug-carrying cargo to local tissues (18, 19). The P3 (CKGGRAKDC) peptide has been reported to bind specifically to WAT vasculature through the membrane protein prohibitin (20). Either Rosi or PGE2 was encapsulated within the peptide-PLGA-PEG-MAL NP using the emulsion solvent evaporation technique, and they are designated as iRGD-NP-Rosi or P3-NP-Rosi, respectively (Fig. 1*B* and Fig. S1). Rosi and PGE2 have adipose tissue browning effects, which can induce adipose tissue transformation and angiogenesis (17, 21). The NPs containing Rosi have an average size of 100 nm (Fig. 1 *C* and *E*). The cumulative drug release profile showed that the NPs continuously release drugs for as long as 40–50 h, with a half-life of 12 h (Fig. 1*D*).

NPs Stimulate SVF in Vitro and Target Adipose Tissue in Vivo. Usually, angiogenic vessels express high levels of integrins, particularly αv and β3 subunits (22). To evaluate whether Rosi-loaded NPs can effectively induce expression of integrins on vascular cells, the stromal vascular fragments (SVF) were isolated from WAT, followed by treatment with Rosi (1 μM) in either solution or nontargeted NP form. Quantitative real-time PCR (qRT-PCR) assay revealed that free Rosi and Rosi-loaded NPs elevated expression of Integrinαv but not Integrinß3 on SVF in vitro (Fig. 2 *A* and *B*). Furthermore, treatment with either Rosi or NP-Rosi stimulated the proliferation of SVF (Fig. 2*C*). We further sorted SVF using the endothelial marker CD31 and stained cells with an Integrinαv antibody. Indeed, we observed up-regulation of Integrinαv with both Rosi and NP-Rosi treatments. These results confirm that Rosi stimulates the expression of Integrinαv at RNA and protein levels in both solution and NP forms, indicating the activation of CD31 positive ECs in vitro.

To examine the distribution of peptide-NP constructs in vivo, fluorescent signals from NPs were analyzed using the IVIS imaging system following injection of FAM-labeled iRGD-NP-Rosi or P3-NP-Rosi into tail veins of mice. One hour after the infusion, FAM-labeled iRGD-NP-Rosi and P3-NP-Rosi had accumulated in inguinal and epididymal WATs, although there was nonspecific accumulation in the livers of all treatment groups due to active liver metabolism (Fig. 2*E*). Only minimal accumulation of nontargeted NP (Ctrl) was detected in WAT. These results suggest that iRGD and P3 peptides facilitate NP homing into WATs in vivo.

NPs Stimulate Angiogenesis and Facilitate Adipose Tissue Transformation in Vivo. We treated wild-type C57BL/6 mice with free Rosi, NP-Rosi,

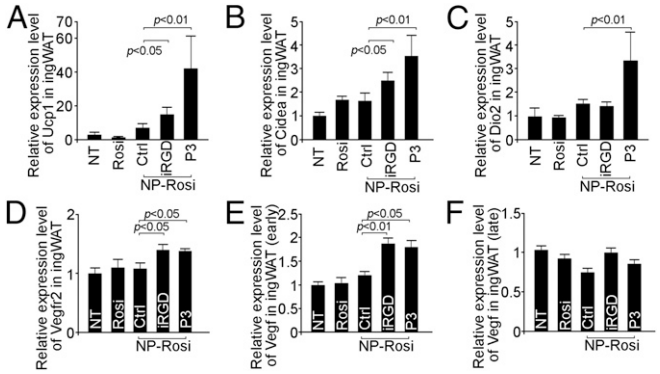

Fig. 4. IRGD- and P3-NP-Rosi up-regulated BAT and angiogenesis markers in inguinal WAT. Total RNAs were isolated from inguinal WAT from various treatment groups. Expression levels of UCP1 (*A*), CIDEA (*B*), DIO2 (*C*), VEGFR2 (*D*), early-stage VEGF (*E*), and late-stage VEGF (*F*) were quantified by qRT-PCR. Data are means ± SEM from three to four mice in each group.

iRGD-NP-Rosi, and P3-NP-Rosi. Fifteen days posttreatment, mice were killed, and complete necropsies were conducted to determine the phenotypical changes in various fat tissues in inguinal and epididymal areas. Both inguinal and epididymal WATs from mice treated with iRGD-NP-Rosi and P3-NP-Rosi appeared more reddish in color than those from control groups (Fig. 2*F*), suggesting more intensive vascularization and possible increased cellular contents in adipocytes. On the cellular level, general histological staining of inguinal WAT with hematoxylin and eosin indicated shrinkage of adipocytes, condensed cellular contents, and transformation of adipocytes (Fig. 3 *A* and *F*). Groups treated with iRGD-NP-Rosi and P3-NP-Rosi showed elevated expression of the BAT marker UCP1 in inguinal WAT compared with control groups (Fig. 3*B*). Furthermore, immunostaining against the EC-specific marker CD31 illustrated increased density of blood vasculature in inguinal WAT of mice treated with iRGD-NP-Rosi and P3-NP-Rosi (Fig. 3 *C* and *E*). Additionally, staining with the independent EC marker Isolectin B4 is consistent with these results (Fig. 3*D*). Because the variable size of adipocytes could affect vascular density, we normalized vessel numbers against adipocyte numbers per optical field and found that the blood vessel numbers were indeed increased more than threefold post iRGD-NP-Rosi and P3-NP-Rosi treatment (Fig. 3*G*). In epididymal WAT, shrinkage of adipocyte size and increase in number of blood vessels were induced by iRGD- and P3-NP-Rosi treatments (Fig. S2*A*). Taken together, these results indicate that iRGD-NP-Rosi and P3-NP-Rosi lead to higher vascular density in comparison with nontargeted NP and free drug control groups, facilitating WAT transformation into brown-like adipose tissue in mice.

NPs Up-Regulate BAT and EC Markers in WATs. We used qRT-PCR to investigate whether the expression patterns of various BAT and EC markers are altered on the molecular level by NP treatment. In inguinal WAT, UCP1 expression was significantly up-regulated by iRGD-NP-Rosi and P3-NP-Rosi (Fig. 4*A*). A marked induction in the expression of another BAT marker, transcriptional coactivator CIDEA (23), was also observed posttreatment with the two targeted NPs (Fig. 4*B*). Notably, treatment with P3-NP-Rosi induced type 2 deiodinase (Dio2) expression, indicating an active brown fat phenotype (Fig. 4*C*). VEGF receptor 2 (VEGFR2), a vascular EC marker, was also up-regulated by treatment with the two peptide-conjugated NPs (Fig. 4*D*). The expression of VEGF was up-regulated in the early stage (4 d) but not in the late stage of treatment (15 d) (Fig. 4 *E* and *F*). Similarly, iRGD-NP-Rosi and P3-NP-Rosi treatments induced higher expression of UCP1, CIDEA, and DIO2 in epididymal WAT (Fig. S2 *B*–*E*).

To evaluate the potential of applying this amplified drug delivery system to other drugs, we treated mice with PGE2-loaded NPs and assessed angiogenesis stimulation and WAT transformation. Similar to Rosi-loaded NPs, iRGD-NP-PGE2 and P3-NP-PGE2 treatments increased the density of CD31-positive blood vasculature about twofold in both inguinal and epididymal WAT (Fig. S3 *A*–*C*). The expression of UCP1 was also up-regulated by those treatments (Fig. 3 *D* and *E*). Those positive results suggest promise for the treatment of obesity with a wide spectrum of encapsulated drugs using this nanomedicine platform with its amplified drug delivery characteristics.

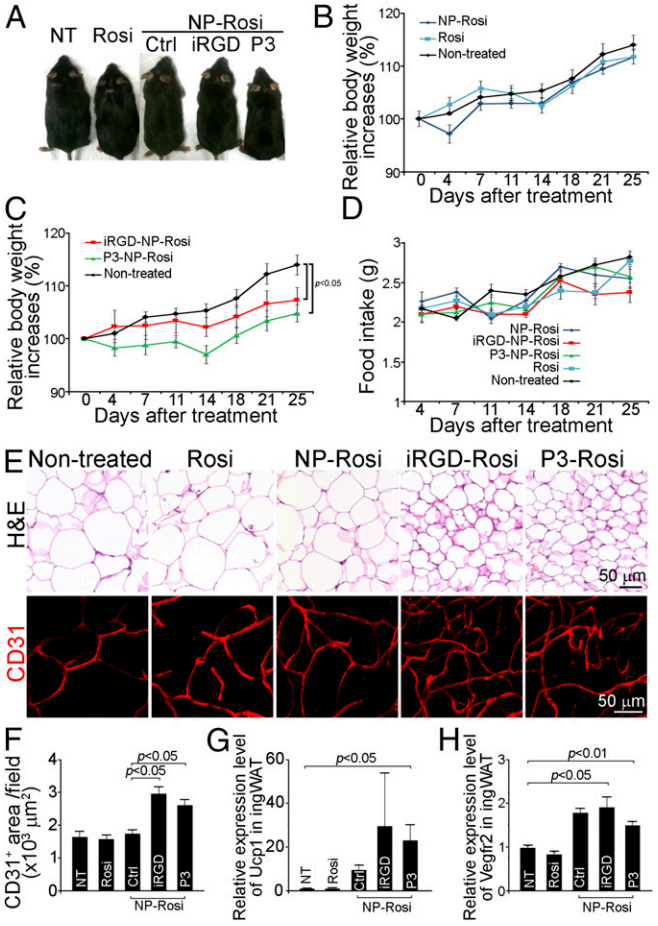

Fig. 5. Antiobesity effect of iRGD-NP-Rosi and P3-NP-Rosi in diet-induced obese (DIO) mice. DIO mice received treatments (intravenously injection at the drug dose of 80 mg/kg, every second day) with Rosi, NP-Rosi, iRGD-Rosi, and P3-NP-Rosi for 25 d. (*A*) Representative mice were photographed at the experiment end point. (*B*) Relative body weight increases of nontreated mice or mice receiving Rosi or NP-Rosi. Data are relative means ± SEM from three to four mice in each group. (*C*) Relative body weight increases of nontreated mice or mice receiving iRGD-NP-Rosi or P3-NP-Rosi. Data are relative means ± SEM from three to four mice in each group. (*D*) Average food intake per mouse per day. Data are means ± SEM from three to four mice in each group. (*E*) Inguinal WATs were stained with hematoxylin and eosin to illustrate histological structure (*Upper*) and immune-stained with anti-CD31 antibody (red; *Lower*) to illustrate vasculature. (Scale bars, 50 μm.) (*F*) Quantification of CD31-positive blood vessels area per optical field. Data are means ± SEM from nine samples in each group. (*G*) Relative expression levels of Ucp1 of inguinal WATs from DIO mice treated with Rosi, NP-Rosi, iRGD-NP-Rosi, and P3-NP-Rosi. Data are means ± SEM from three to four mice in each group. (*H*) Relative expression levels of Vegfr2 of inguinal WATs from DIO mice treated with Rosi, NP-Rosi, iRGD-NP-Rosi, and P3-NP-Rosi. Data are means ± SEM from three to four mice in each group.

Enhanced Effect of Targeted NPs on Inhibition of Obesity Development in DIO Mice. Because adipose tissue transformation and angiogenesis can be initiated by treatment with the two peptide-NP-Rosi constructs, we investigated whether such treatment could regulate metabolism, inhibit the development of obesity, or demonstrate any therapeutic effects in obese mice. We used the high-fat diet induced obese model to assess the possible effect of the two peptide-NP-Rosi constructs on body weight, tissue histology, and molecular expression profiles. There was no difference in body weight gain between the mice treated with Rosi (in solution and nontargeted NP forms) and nontreated obese mice (Fig. 5 *A* and *B*). In contrast, both targeted NPs significantly inhibited body weight gain by about 10% in DIO mice 25 d posttreatment (Fig. 5 *A* and *C*; $P < 0.05$). Notably, mice from different treatment groups demonstrated similar food intakes (Fig. 5*D*). H&E staining revealed shrinkage of adipocytes in WAT by both targeted NP treatments (Fig. 5*E*). CD31-positive adipose tissue vasculature was markedly increased (about twofold) in mice receiving iRGD-NP-Rosi and P3-NP-Rosi treatments compared with control groups (Fig. 5 *E* and *F*). In addition, molecular expression UCP1 and VEGFR2 were up-regulated by both peptide-functionalized NP treatments (Fig. 5 *G* and *H*). These findings indicate that both iRGD-NP-Rosi and P3-NP-Rosi exerted significant antiobesity effects in a DIO mouse model by activating adipose tissue transformation and angiogenesis.

Lipid and Carbohydrate Metabolism in DIO Mice. After DIO mice were treated for 25 d and fasted for 5 h, their serum was analyzed for serological parameters. As shown in Fig. 6*A*, DIO mice receiving either iRGD-NP-Rosi or P3-NP-Rosi showed a significant 30% reduction in serum cholesterol compared with the nontreatment group. Furthermore, both iRGD-NP-Rosi and P3-NP-Rosi treatments resulted in statistically ($P < 0.05$) marked decreases in serum triglyceride level compared with the nontreatment (NT) group (Fig. 6*B*). There was no significant difference in the serum levels of free fatty acids (FFAs) and glucose among the groups (Fig. 6 *C* and *D*). However, free Rosi and the nontargeted version of NP reduced the production of serum insulin threefold, whereas iRGD-NP-Rosi and P3-NP-Rosi resulted in even greater reduction (Fig. 6*E*). We also calculated the indirect insulin resistance index (IR = Insulin × FFA), which was lowest in the mice receiving both targeted NP treatments, indicating elevated insulin sensitivity (Fig. 6*F*).

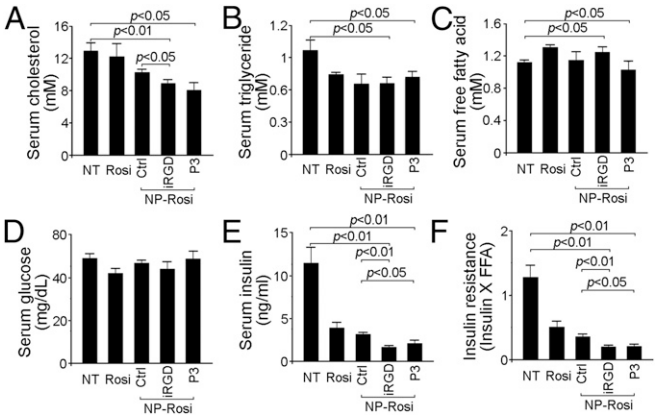

Fig. 6. BAT, vascular markers, and serological parameters from DIO mice were altered by of iRGD-NP-Rosi and P3-NP-Rosi treatments. Quantification of serum levels of cholesterol (*A*), triglyceride (*B*), free fatty acid (FFA) (*C*), glucose (*D*), and insulin (*E*) from fasting DIO mice treated with Rosi, NP-Rosi, iRGD-NP-Rosi, and P3-NP-Rosi. Data are means ± SEM from three to four mice in each group. (*F*) Insulin resistance was calculated as insulin level × FFA level. Data are means ± SEM from three to four mice in each group.

Preliminary Effect of NP and NP-Peptide Constructs on Food Intake and Body Weight. To evaluate the preliminary safety profile of the NPs, we treated C57BL/6 mice with NP or iRGD-NP (no encapsulated Rosi) for 3 wk and observed if the nanoparticle constructs might affect the food intake and body weight of mice. We did not detect any changes in regard to body weight (Fig. S4*A*) or food intake (Fig. S4*B*) of the treated mice. These preliminary data suggested the limited effect of NP constructs on food consumption and body weight we tested. Thus, the observed effects of adipose tissue transformation and obesity inhibition by peptide-NP-Rosi are likely mediated by the targeted delivery of Rosi.

Discussion

The regulators of the intercalated feedback loop, controlling both food intake and body weight, include adipose tissues, the brain, pancreas, muscles, vasculature, and the gastrointestinal tract (4, 8). Adipose tissues and vasculature are the most plastic, growing, regressing, and remodeling throughout the life span (2). Thus, the manipulation of adipose tissues and vasculature may be a useful therapeutic strategy for treating metabolic diseases including obesity and diabetes. Previous studies in mouse and monkey models have shown that ligand-directed peptidomimetic compounds can induce apoptosis within the blood vasculature of white adipose tissue and result in rapid weight loss and improved insulin resistance (10, 20). A few other studies demonstrated that methionine aminopeptidase inhibitors, fumagillin and beloranib, could induce sustained weight reduction by reducing the production of new fatty acids in the liver and reducing the pathological angiogenesis in adipose tissue (24, 25). Other groups have also demonstrated that angiogenesis inhibitors such as TNP-470, angiostatin, and endostatin exhibited antiobesity effects by inhibiting blood vessel growth in preclinical models (3, 5). However, this line of inquiry has been challenged by the fact that energy expenditure requires active angiogenesis (6). In the current study, we show that angiogenesis activation accompanied adipose tissue transformation from WAT into brown-like adipose tissue, which supports the concept that stimulation of angiogenesis can facilitate the switch of adipose tissues to metabolically active status.

In obese individuals, significant body mass is composed of WAT, whereas BATs are concentrated in the neck, supraclavicular regions, and mediastinum (12, 26). To modulate WAT angiogenesis, a relatively large dose of drug is required when using conventional drug delivery approaches, which might in turn lead to off-target drug accumulation in other organs and potential side effects. Selective delivery of angiogenesis modulators to massively expanded adipose tissues using NPs may minimize off-target adverse effects and circumvent the concerns associated with angiogenesis-targeted therapy. Targeted NPs have shown significant therapeutic potential in both research and clinical settings and are widely expected to change the landscape of pharmaceutical and biotechnology industries for the foreseeable future (27–29).

Here we used two peptides, iRGD and P3, targeted to angiogenic vessels in adipose tissues. Recent evidence has reported that iRGD binds to integrin αv on angiogenic ECs and is further cleaved into the CRGDK fragment. This fragment binds to neuropilin-1, which facilitates the penetration of the drug-loaded cargo into local tissues (18, 30). Another study used a phage display technique to show that P3 can be specifically recognized by the WAT vasculature through the membrane protein prohibitin (20). By conjugation of the aforementioned targeting peptides to NPs, we developed a robust drug delivery platform that carries hydrophobic adipose tissue browning agents (Rosi) and investigated their antiobesity effects as a proof of concept. With treatments of these targeted NPs loaded with Rosi, the activation of both transformation and angiogenesis creates a positive feedback loop that enables more NP homing into local adipose tissue,

amplifying the WAT browning process. We demonstrate that the targeted NPs exhibited greater accumulation in WAT and anti-obesity effects compared with the free drug and the nontargeted NP. In addition, we observed similar angiogenesis stimulation and WAT transformation both in vitro and in vivo using targeting NPs loaded with another adipose tissue browning agent (PGE2).

Rosi plays polarized roles in modulating angiogenesis under pathological and physiological conditions. Previous study showed that Rosi acted as a potent inhibitor in tumor angiogenesis (31), whereas another study together with data from our study demonstrated Rosi's role as an angiogenesis stimulator in adipose tissue transformation (15). In clinical application, Rosi is linked with increased risk of heart attack, stroke, and bone fractures. The current study used Rosi as a proof of concept to demonstrate the feasibility of our nanoparticles. The benefit and risk profiles of Rosi have not been assessed in our study. Thus, the therapeutic application of Rosi should be cautious.

It is worthwhile to note that the encapsulated drug candidates are not limited to Rosi or PGE2. For instance, specifically tailored siRNAs or functional proteins such as FGF21 (32) can also be loaded into the targeted nanocarriers to regulate adipose tissue transformation and angiogenesis. Alternatively, it is possible to encapsulate multiple therapeutic agents into the same NP (33), which may offer synergistic effects in combination therapy.

In conclusion, we provide evidence of the validity of an angiogenesis-targeted nanomedicine approach to deliver adipose tissue browning agents and simultaneously stimulate angiogenesis in WAT. The resulting high vascular density allows greater drug accumulation in WAT, which produces a positive feedback loop, accelerating the transformation of WAT into BAT. Furthermore, targeted NP-mediated weight gain inhibition was confirmed in the DIO mouse model, which was less evident in treatments with nontargeted NP and free drug formulations. This strategy of combined targeted nanomedicine for angiogenesis stimulation could potentially open the way toward effective treatments for obesity and other metabolic diseases.

Materials and Methods

All animal studies were approved by the Committee on Animal Care, Massachusetts Institute of Technology. Materials and procedures for the synthesis and characterization of PLGA-*b*-PEG-Peptide conjugates and NPs can be found in *SI Materials and Methods*. The NMR analysis of PLGA-*b*-PEG-Peptide (Fig. S5), release of Rosi from the NPs, immunohistochemistry, quantitative real-time PCR, animal experiments, and statistical analyses are described in *SI Materials and Methods*.

ACKNOWLEDGMENTS. We thank Dr. B. Spiegelman, Dr. H. Yin, Dr. O. Veiseh, and Dr. N. Betrand for helpful discussions. This work is in part supported by National Institutes of Health (NIH) Grants EB016101-01A1 and EB006365 (to R.L.); Koch–Prostate Cancer Foundation Award in Nanotherapeutics (to R.L. and O.C.F.); and NIH R01 Grant EB015419 (to O.C.F). Y.X. is supported by the Swedish Research Council. X.X. acknowledges postdoctoral support from an NIH National Research Service Award (1F32CA168163-03).

1. Folkman J (1995) Angiogenesis in cancer, vascular, rheumatoid and other disease. *Nat Med* 1(1):27–31.
2. Cao Y (2007) Angiogenesis modulates adipogenesis and obesity. *J Clin Invest* 117(9):2362–2368.
3. Rupnick MA, et al. (2002) Adipose tissue mass can be regulated through the vasculature. *Proc Natl Acad Sci USA* 99(16):10730–10735.
4. Cao Y (2010) Adipose tissue angiogenesis as a therapeutic target for obesity and metabolic diseases. *Nat Rev Drug Discov* 9(2):107–115.
5. Bråkenhielm E, et al. (2004) Angiogenesis inhibitor, TNP-470, prevents diet-induced and genetic obesity in mice. *Circ Res* 94(12):1579–1588.
6. Xue Y, et al. (2009) Hypoxia-independent angiogenesis in adipose tissues during cold acclimation. *Cell Metab* 9(1):99–109.
7. Finucane MM, et al.; Global Burden of Metabolic Risk Factors of Chronic Diseases Collaborating Group (Body Mass Index) (2011) National, regional, and global trends in body-mass index since 1980: Systematic analysis of health examination surveys and epidemiological studies with 960 country-years and 9·1 million participants. *Lancet* 377(9765):557–567.
8. Friedman JM (2009) Obesity: Causes and control of excess body fat. *Nature* 459(7245):340–342.
9. Colman E, et al. (2012) The FDA's assessment of two drugs for chronic weight management. *N Engl J Med* 367(17):1577–1579.
10. Barnhart KF, et al. (2011) A peptidomimetic targeting white fat causes weight loss and improved insulin resistance in obese monkeys. *Sci Transl Med* 3(108):108ra112.
11. Nedergaard J, Bengtsson T, Cannon B (2007) Unexpected evidence for active brown adipose tissue in adult humans. *Am J Physiol Endocrinol Metab* 293(2):E444–E452.
12. Virtanen KA, et al. (2009) Functional brown adipose tissue in healthy adults. *N Engl J Med* 360(15):1518–1525.
13. Hrkach J, et al. (2012) Preclinical development and clinical translation of a PSMA-targeted docetaxel nanoparticle with a differentiated pharmacological profile. *Sci Transl Med* 4(128):128ra39.
14. Foellmi-Adams LA, Wyse BM, Herron D, Nedergaard J, Kletzien RF (1996) Induction of uncoupling protein in brown adipose tissue. Synergy between norepinephrine and pioglitazone, an insulin-sensitizing agent. *Biochem Pharmacol* 52(5):693–701.
15. Gealekman O, et al. (2008) Enhanced angiogenesis in obesity and in response to PPARgamma activators through adipocyte VEGF and ANGPTL4 production. *Am J Physiol Endocrinol Metab* 295(5):E1056–E1064.
16. Cipolletta D, et al. (2012) PPAR-γ is a major driver of the accumulation and phenotype of adipose tissue Treg cells. *Nature* 486(7404):549–553.
17. Madsen L, et al. (2010) UCP1 induction during recruitment of brown adipocytes in white adipose tissue is dependent on cyclooxygenase activity. *PLoS One* 5(6):e11391.
18. Sugahara KN, et al. (2009) Tissue-penetrating delivery of compounds and nanoparticles into tumors. *Cancer Cell* 16(6):510–520.
19. Teesalu T, Sugahara KN, Ruoslahti E (2013) Tumor-penetrating peptides. *Front Oncol* 3:216.
20. Kolonin MG, Saha PK, Chan L, Pasqualini R, Arap W (2004) Reversal of obesity by targeted ablation of adipose tissue. *Nat Med* 10(6):625–632.
21. Tiraby C, et al. (2003) Acquirement of brown fat cell features by human white adipocytes. *J Biol Chem* 278(35):33370–33376.
22. Weis SM, Cheresh DA (2011) αV integrins in angiogenesis and cancer. *Cold Spring Harb Perspect Med* 1(1):a006478.
23. Zhou Z, et al. (2003) Cidea-deficient mice have lean phenotype and are resistant to obesity. *Nat Genet* 35(1):49–56.
24. Joharapurkar AA, Dhanesha NA, Jain MR (2014) Inhibition of the methionine aminopeptidase 2 enzyme for the treatment of obesity. *Diabetes Metab Syndr Obes* 7:73–84.
25. Scroyen I, Christiaens V, Lijnen HR (2010) Effect of fumagillin on adipocyte differentiation and adipogenesis. *Biochim Biophys Acta* 1800(4):425–429.
26. Lidell ME, et al. (2013) Evidence for two types of brown adipose tissue in humans. *Nat Med* 19(5):631–634.
27. Farokhzad OC, Langer R (2009) Impact of nanotechnology on drug delivery. *ACS Nano* 3(1):16–20.
28. Kamaly N, Xiao Z, Valencia PM, Radovic-Moreno AF, Farokhzad OC (2012) Targeted polymeric therapeutic nanoparticles: Design, development and clinical translation. *Chem Soc Rev* 41(7):2971–3010.
29. Zhang XQ, et al. (2012) Interactions of nanomaterials and biological systems: Implications to personalized nanomedicine. *Adv Drug Deliv Rev* 64(13):1363–1384.
30. Sugahara KN, et al. (2010) Coadministration of a tumor-penetrating peptide enhances the efficacy of cancer drugs. *Science* 328(5981):1031–1035.
31. Panigrahy D, et al. (2002) PPARgamma ligands inhibit primary tumor growth and metastasis by inhibiting angiogenesis. *J Clin Invest* 110(7):923–932.
32. Hondares E, et al. (2010) Hepatic FGF21 expression is induced at birth via PPARalpha in response to milk intake and contributes to thermogenic activation of neonatal brown fat. *Cell Metab* 11(3):206–212.
33. Jia J, et al. (2009) Mechanisms of drug combinations: Interaction and network perspectives. *Nat Rev Drug Discov* 8(2):111–128.
34. Xue Y, et al. (2011) PDGF-BB modulates hematopoiesis and tumor angiogenesis by inducing erythropoietin production in stromal cells. *Nat Med* 18(1):100–110.